# Calculation of the $M_{23}$ magneto-optical absorption spectrum of ferromagnetic nickel

J. L. Erskine*
*Department of Physics, University of Illinois, Urbana, Illinois 61801*

E. A. Stern†
*Department of Physics, University of Washington, Seattle, Washington 98195*

(Received 28 April 1975)

The $M_{23}$ magneto-optical absorption spectrum of ferromagnetic nickel is calculated using an approach similar to the component state-density method that has been successfully used in obtaining valence-band emission and absorption x-ray spectra of metals. The $M_{23}$ magneto-optical effects result predominantly from spin-orbit splitting of the $3p$ core state in conjunction with the final $d$-state spin polarization. The calculated spectrum exhibits features that are directly related to electronic structure parameters including the $3p$ core spin-orbit splitting, and the unfilled $d$-band spin polarization. Temperature variations in the magneto-optical structure can be used to determine separately the exchange-splitting variation and spin-wave excitation contributions to the decrease in the magnetization. Experimental verification of these predictions should provide insight into the applicability of the Stoner model to ferromagnetic nickel and may be helpful in resolving some of the apparently conflicting results of other experimental probes of the spin polarization near the Fermi level in nickel.

## I. INTRODUCTION

Our present understanding of ferromagnetism is based on simple conceptual models. In 1907, Weiss[1] proposed the existence of magnetic moments which are coupled in a ferromagnetic metal by a macroscopic field—the well-known molecular-field model. Refinements of the Weiss model lead to two divergent viewpoints concerning the nature of the magnetic moments in ferromagnetic materials. These moments can be associated with the highly localized unpaired spins (the Heisenberg picture[2]) or the unequally populated spin-up and spin-down conduction bands (the Stoner picture[3]).

In the last few years a variety of experiments have been performed on various magnetic materials in attempts to provide a better basis for these models and to test predictions based on them. Recently, application of the Stoner model to transition-metal ferromagnets has received considerable attention. The fractional moments found in these metals have encouraged the use of a Stoner picture in analysis and interpretation of experimental data for a majority of the measurements. In most cases, experimental results obtained for transition metals have been found to be compatible with the Stoner model, and some results provide strong support for it. On the other hand, there are several experiments that yield results that do not appear to be consistent with the Stoner model. Gutzwiller[4] has summarized these experiments and the resulting implications.

Galvanomagnetic and de Haas–van Alphen measurements conducted on transition-metal ferromagnets, in general, support the Stoner model description of the ground state. Recent review papers by Gold[5] and Cracknell[6] discuss Fermi-surface experiments from the viewpoint of how well they support the split-band picture. These studies have established topologically distinct minority and majority spin Fermi surfaces for Fe and Ni that agree well with a Stoner band-model description of the ground state. On the other hand, attempts to measure Stoner splitting effects on Fermi-surface geometry by studying de Haas–van Alphen frequency shifts as a function of temperature lead to the conclusion that the band splitting does not vary with temperature in proportion to the total magnetization[5] as the Stoner model assumes.

Magneto-optical studies of transition-metal ferromagnets covering the 0.5- to 5.5-eV energy range also support the Stoner model. The spectral dependence of magneto-optical absorption of nickel at low frequencies has been attributed to transitions involving minority spin bands near the Fermi level.[7] Conclusions derived from an analysis of magneto-optical spectra based on relatively simple band models[7] are now supported by direct computations of the magneto-optical spectra from ferromagnetic band calculations.[8] These results confirm the relationship between structure in experimental data and gross features of the electronic structure such as the net spin polarization and density of states that were established using the simple models. The detailed calculations also verify that the independent particle approach produces reasonable agreement between measured and computed magneto-optical spectra in the visible near-uv range. Magneto-optical studies to date do not prove that the Stoner splitting exists, although as will be pointed out in this paper, care-

fully conducted temperature-dependent studies of magneto-optical spectra appear to offer one of the most sensitive and direct probes for this splitting.

Other experimental evidence in favor of applicability of the Stoner model to transition-metal ferromagnets include elastic neutron scattering and the analysis of magnetic moment and photoemission data. The neutron-scattering experiments[9] provide information about the spatial distribution of the magnetic moment within the atom, and these results have been shown to be compatible with band-theory predictions. The exchange splittings $\Delta E = (n_\uparrow - n_\downarrow)I$ estimated by combining data from magnetic-moment measurements and density-of-states data obtained from photoemission measurements yield an effective exchange integral $I$ of 0.5 eV for Ni, Co, and Fe, in general agreement with predictions based on the Stoner framework.[10]

In spite of the compelling evidence in favor of the Stoner model, in the last few years several experiments have produced results that may be interpreted as posing a challenge to the validity of the model and its predictions. Early attempts to directly measure shifts in energy bands due to exchange splitting by studying temperature-induced shifts in the photoemission spectrum of nickel above and below its Curie temperature yielded null results.[11] Subsequent experiments have measured a systematic shift with temperature, but the observed shift is considerably less than what one would expect.[12] Recent neutron-diffraction studies have also indicated that the exchange splitting may not go to zero at the Curie temperature.[13] Theoretical calculations have since indicated how this result can still be made consistent with the Stoner model.[14]

The spin-polarized photoemission experiments[15] and spin-dependent tunneling measurements,[16] particularly the results for Ni, provide a much stronger contrast between observed results and Stoner model predictions. In the photoemission experiments, electrons photoemitted from a magnetically saturated sample are analyzed for their spin polarization in a Mott scattering device. The results of spin-polarized emission experiments and other related experiments have been reviewed by Gutzwiller[4] and by Siegmann.[17] The conclusions appear to call for new models for the magnetic state and for electron emission processes. One of the most striking apparent contradictions of Stoner model predictions is found in the spin-polarized photoemission experiments in nickel. The spin-polarized photoemission experiments measure a positive sign for the spin polarization of electrons near the Fermi level in nickel. Application of the Stoner model to calculated bands for nickel, or to band density-of-states models established by photoemission, results in a prediction opposite to that measured by the spin-polarized photoemission and tunneling results. That is, when the majority and minority spin bands of nickel are shifted by the energy necessary to account for the observed magnetic moment, the minority spin $d$-band density of states near the Fermi level dominates. This feature alone has attracted a significant amount of attention that has focused primarily on attempts to reconcile the positive spin polarization for nickel within the framework of the Stoner picture.[18] The interpretation of the spin-polarized photoemission and tunneling experiment have been criticized as not measuring in any simple way the polarization of the band electrons.[19] At present, the only thing that is clear is that more independent and straightforwardly interpretable measurements are required.

Magneto-optic measurements can contribute significantly to our understanding of this aspect of the magnetism of transition metals, in particular Ni, which has recently attracted much attention. De Haas–van Alphen measurements in Fe have shown a related fact, namely, that the decrease in magnetization at low temperatures does not appear to be accompanied by a corresponding decrease in the Stoner exchange splitting.[5,20] This result and the related neutron measurements[13] result can be reconciled with the Stoner model.

To do so, consider a long-wavelength spin excitation or magnon. If the wavelength of the magnon is large enough, it can be treated classically as a spatially varying spin wave. Consider a classical spin wave that has an amplitude equal to the static magnetization. This corresponds to the coherent excitation of an extremely large number of magnon excitations. Locally the magnetization is always the static one, and for a long enough wavelength it is clear that locally the Stoner exchange is always the same and equal to the value of the unperturbed magnet. Yet the net magnetization averaged over a wavelength will be zero. Thus the net magnetization will be decreased by long-wavelength magnons without affecting the Stoner exchange splitting.

One must therefore distinguish between the two distinct mechanisms that contribute to a decrease in net magnetization. One is a magnon or spin-wave excitation and the other is a decrease in the exchange splitting. As described in Sec. III, magneto-optical measurements have the exciting capability of determining these two contributions separately.

In this paper we calculate the magneto-optical absorption spectrum associated with $M_{23}$ edge of ferromagnetic nickel and discuss how measurements of this spectrum offer an opportunity to determine the electronic structure of the $d$ bands just above the Fermi energy. The information that can

be obtained experimentally include the spin polarization of states just above the Fermi energy, the $3p$ core state spin-orbit splitting, the width of the minority spin $d$ band above the Fermi level, and perhaps its shape. A temperature-dependence study of the $M_{23}$ magneto-optical spectrum should permit a definitive measurement of the exchange splitting of magnetic bands in nickel as a function of temperature. In short, magneto-optical techniques can be an important supplement to more standard methods of spectroscopic studies of solids in the uv and x-ray region.

In Sec. II we briefly outline the main features of magneto-optical spectroscopy of ferromagnetic metals with a few comments related to extension of this experimental technique into the far-uv and soft-x-ray region. Section III contains a calculation of the $M_{23}$ magneto-optical absorption of ferromagnetic nickel, and Sec. IV summarizes the results and presents conclusions, including a brief discussion of the feasibility of experimental verification of the predictions.

## II. MAGNETO-OPTICAL EFFECTS IN MAGNETIC METALS

Magneto-optical behavior of ferromagnetic metals is dominated by the magneto-optic Kerr effect (MOKE) mechanism. MOKE is produced by the combined effects of spin-orbit coupling and net spin polarization. The observed phenomena depends on which of three possible configurations is used. The configurations, defined by the relative orientation of the magnetization $\vec{M}$ and the plane of incidence are (a) the polar configuration in which $\vec{M}$ is perpendicular to the reflecting surface; (b) the longitudinal configuration in which $\vec{M}$ is parallel to the plane of incidence and to the sample surface; and (c) the transverse configuration in which $\vec{M}$ is perpendicular to the plane of incidence and parallel to the plane of the sample surface.

In the polar and longitudinal configurations, plane-polarized incident light becomes elliptically polarized, having the major axis of polarization rotated with respect to the original polarization axis. In the transverse configuration, the intensity of $p$-polarized light reflected at oblique incidence changes slightly upon reversal of the magnetization. In all cases, the magnitude of the observed effect, i.e., the rotation and ellipticity, or the change in intensity, is proportional to $\vec{M}$ and vanishes above the Curie temperature.

When the sample can be assumed optically isotropic for $\vec{M}=0$, and with $\vec{M}$ chosen to lie along the the $\tilde{z}$ direction, the conductivity of the solid $\tilde{\sigma}(\omega)$ describing both optical and magneto-optical behavior becomes[21]

$$\tilde{\sigma}(\omega)=\begin{pmatrix}\sigma_{xx} & \sigma_{xy} & 0\\ -\sigma_{xy} & \sigma_{xx} & 0\\ 0 & 0 & \sigma_{zz}\end{pmatrix}. \tag{1}$$

In Eq. (1) the diagonal terms $\sigma_{xx}(\omega)$ and $\sigma_{zz}(\omega)$ are even in $\vec{M}$, and thus to first order independent of $\vec{M}$, describing the ordinary optical behavior of the solid. The off-diagonal terms $\sigma_{xy}(\omega)$ are odd in $\vec{M}$ and thus to first order are proportional to $\vec{M}$ and describe the MOKE. Both diagonal and off-diagonal terms are complex quantities, $\sigma_{ij}=\sigma_{ij}^{(1)}+i\sigma_{ij}^{(2)}$. The absorptive component of diagonal terms $\sigma_{xx}^{(1)}$ is proportional to the sum of absorption of left and right circularly polarized light (RCP and LCP). The absorptive component of off-diagonal terms $\sigma_{xy}^{(2)}$ is proportional to the difference in absorption of LCP and RCP components.[21] The change in role of real and imaginary components in describing absorption results from the first-order dependence of $\sigma_{xy}(\omega)$ on the spin-orbit coupling and the fact that the spin-orbit operator is imaginary. In the visible and near-uv range magneto-optical absorption is typically of the order of $10^{-3}$ of ordinary optical absorption.

This same macroscopic description of magneto-optical effects remains valid in the uv and soft-x-ray region. Microscopic calculations based on the dipole approximation remain valid, and the standard optical range Fresnel-Maxwell formulas relating optical and magneto-optical phase shifts, reflection coefficients, and transmission coefficients are also applicable since the wavelength is much longer than the dimensions of the atomic state that is excited.

The dependence of MOKE on the spin polarization renders this spectroscopic method a particularly useful probe for electronic structure of magnetic metals: The structure in MOKE spectra can be unambiguously associated with magnetized electron bands.[22] In addition, the off-diagonal components of $\tilde{\sigma}(\omega)$ can have either a positive or negative sign that depends directly on the net spin-polarization of electrons responsible for magneto-optic absorption at a given wavelength.[22] Thus the MOKE provides a direct probe of the spin polarization of magnetic bands as a function of energy.

Formal expressions for calculating magneto-optical absorption have been given by various authors.[21,23] Neglecting damping and $k$ dependence, the absorptive component of $\sigma_{xy}(\omega)$ is given by[21]

$$\sigma_{xy}^{(2)}(\omega)=\frac{e^2}{2m^2\hbar}\sum_{\alpha\beta}\left(\frac{|\pi_{\alpha\beta}^{-}|^2}{(\omega_{\alpha\beta}^{-})^2-\omega^2}-\frac{|\pi_{\alpha\beta}^{+}|^2}{(\omega_{\alpha\beta}^{+})^2-\omega^2}\right), \tag{2}$$

where $|\pi_{\alpha\beta}^{+}|^2$ represent the square of matrix elements of the momentum operator

$$\pi=p+(e/c)A+(1/2mc^2)\sigma\times\nabla.$$

The sum extends over all occupied states $\beta$ and empty states $\alpha$. It is sufficient for our purposes for both the wave functions $|\alpha\rangle$ and $|\beta\rangle$ and the energy denominators $\omega^{\pm}_{\alpha\beta}$, corresponding to energy differences between the states $\alpha$ and $\beta$ coupled by transitions for LCP and RCP light, to be calculated to first order in the spin-orbit coupling parameters.

When discussing the MOKE, we are only interested in optical effects associated with a net spin polarization, so we assume $H=0$ and $M\neq 0$. In this case, a nonzero value of $\sigma^{(2)}_{xy}(\omega)$ is produced when spin-orbit effects cause a failure of the two terms, being subtracted in Eq. (2), to cancel. Three separate mechanisms can cause this to occur. In magnetic metals where orbital quenching is strong, and at ir, visible, and near-uv wavelengths where transitions are restricted to initial and final states described by Bloch waves, magneto-optical effects are best described by considering the perturbation of spin-orbit coupling on the matrix elements $|\pi^{\pm}_{\alpha\beta}|^2$, either through spin-orbit effects on the wavefunctions $|\alpha\rangle$ and $|\beta\rangle$ or by the direct contribution of spin-orbit coupling to the momentum operator $\pi$. At higher energies where initial states can be a core state, having a spin-orbit splitting large compared with the spin-orbit splitting of the final-state conduction band, magneto-optical absorption is dominated by the energy shift of LCP and RCP transitions produced by the spin-polarization of the conduction band and spin-orbit splitting of the core state. In this case, it is the product of the final-state spin polarization and the initial-state spin-orbit splitting that destroys the cancelation of the terms in Eq. (2).

It is interesting to compare this type of excitation with the situation at lower energies where magneto-optical effects are produced by transitions between a pair of bands rather than by a narrow core level and a band. If we assume that orbital quenching is not complete in a case where a pair of bands produce magneto-optical effects, we can use the same mechanism involving the spin-orbit splitting to illustrate a basic difference between the two cases where (a) either the initial or final state is highly localized with strong spin-orbit coupling, and (b) where both states are conduction-band states.

In case (b) involving band-to-band transitions, the bandwidth of the joint density of states is typically much wider than the spin-orbit splitting, and in this case, a partial cancellation of the $\Delta M=\pm 1$ matrix elements results in the reduction of the strength of magneto-optical effects, roughly in proportion to $\Delta E_{\text{spin-orbit}}/\Delta E_{\text{bandwidth}}$.[22]

In the case of excitations from a core level having a spin-orbit splitting large in comparison with the effective width of the unoccupied band, as is the the somewhat unique case for nickel, the cancelation is small, and strong magneto-optical effects, somewhat analogous to the splitting of atomic lines, can be observed. Broadening by many-body mechanisms can reduce the amplitudes, but for the $M_{23}$ edge of nickel (as will be shown in Sec. III) these effects should not be too large, and the striking magneto-optical spectra predicted should be produced.

## III. CALCULATION

In this section, the $M_{23}$ magneto-optical absorption spectrum for nickel is calculated using an approach analogous to the component state-density method that has been successfully used in obtaining valence-band emission and absorption x-ray spectra of metals.[24] This approach is based on the single-particle model of optical transitions from a core state of prescribed symmetry described by atomic wave functions into component conduction-band states with symmetry corresponding to allowed optical transitions. The band wave functions and state densities are obtained from band calculations, and in the calculation of matrix elements the $k$ dependence of transition probabilities is neglected. Although, generally, the energy variation of the matrix elements can be taken into account, the variation that occurs in nickel over the energy range corresponding to unfilled $d$ bandwidths is very small,[25] and we therefore neglect this effect in our calculations.

The utility and limitations of the local density-of-states approach to x-ray absorption calculations have been fairly well established. In the case of the transition metals, and for nickel, in particular, which has been studied extensively by x-ray methods, this computational approach has produced $K$ and $L$ absorption spectra that are in reasonably good agreement with experimental data.[25] The $M$ absorption in nickel appears to be more strongly influenced by many-body effects as described briefly below.

Typical results for the case of nickel are illustrated in Figs. 1 and 2. In Fig. 1, the $s$-, $p$-, and $d$-character component densities for minority and majority spin bands have been obtained from computed bands.[25] In Fig. 2, the $d$-state density above the Fermi level is compared with the separated $M_2$ and $M_3$ components determined from the measured $M$ absorption spectrum of nickel.[26] The modulation of the $M_2$ and $M_3$ spectrum does not reflect the sharp and large density-of-states contribution at the edge. The cause for this can be explained by lifetime effects which are apparent in the rate of rise in absorption at the edge, which corresponds to about a 1.5-eV lifetime broadening.

Lifetime broadening effects can be included into the component density-of-states model by introduc-

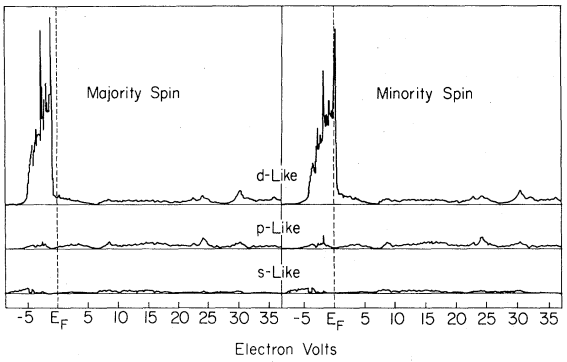


FIG. 1. Component state densities for nickel (Ref. 25).

ing an appropriate relaxation time, but a more complete accounting of other many-body effects lies outside of the scope of this paper. Recent x-ray photoemission data on Ni also indicated lifetime broadening effect[27] of the order of 1.5 eV. In addition to neglecting other kinds of many-body effects than those that can be accounted for by lifetime broadening, we also neglect the electron-hole interaction. Electron-hole interaction effects can be quite large, and are responsible for the rapid rise of absorption at edges and possibly other kinds of prominent structures such as white lines.[28] Yet on top of all of these effects, one expects that the density of states will introduce a modulation, for the $M_{23}$ edges of Ni, as is discernible in Fig. 2 and seen in other cases also. It is this part of both the ordinary and magneto-optic absorption that we calculate here.

We wish to calculate the magneto-optical absorption produced by electric dipole transitions from the $3p$ doublet to the unfilled portion of the $d$ bands. As pointed out in the Sec. II, in nickel, the $3p$ core state spin-orbit splitting is large in comparison with spin-orbit splitting associated with the $d$ states, and this results in the MOKE absorption associated with initial $3p$ states to be produced primarily by the $3p$-state spin-orbit splitting and the final $d$-state spin polarization.

In this case, the matrix elements in Eq. (2), carried to first order in the product of spin polarization times spin-orbit coupling, become standard dipole matrix elements between initial states $\beta$ corresponding to the $3p$ doublet and final states $\alpha$ representing spin-polarized $d$-character conduction-band states above the Fermi level:

$$|\pi^{\pm}_{\alpha\beta}|^2 = \omega^2 m^2 |\langle\alpha|x \pm iy|\beta\rangle|^2. \quad (3)$$

The angular part of normalized $3p$ doublet wave functions are listed in Table I along with the $d$-

TABLE I. Character of the angular and spin portions of states pertinent to the calculation of $M_{23}$ optical and magneto-optical absorption. Spin orientation along the $z$ axis is denoted by + or − signs inside the parentheses. First subscripts on the angular eigenstates denote the $l$ value and the second subscript the $m$ value.

| Core state | | Character |
|---|---|---|
| $3P_{1/2}$ | $m=\frac{1}{2}$ | $\frac{1}{3}\sqrt{3}\,[(+)Y_{10}-\sqrt{2}(-)Y_{11}]$ |
| | $m=-\frac{1}{2}$ | $\frac{1}{3}\sqrt{3}\,[(-)Y_{10}-\sqrt{2}(+)Y_{1-1}]$ |
| | $m=\frac{3}{2}$ | $(+)Y_{11}$ |
| | $m=\frac{1}{2}$ | $\frac{1}{3}\sqrt{3}\,[\sqrt{2}(+)Y_{10}+(-)Y_{11}]$ |
| | $m=-\frac{1}{2}$ | $\frac{1}{3}\sqrt{3}\,[\sqrt{2}(-)Y_{10}+(+)Y_{1-1}]$ |
| | $m=-\frac{3}{2}$ | $(-)Y_{1-1}$ |

| Band-state representation | $d$ character | Weight |
|---|---|---|
| $X_{5\downarrow}$ | $(-)Y_{2\pm1}$ | $\frac{2}{3}$ |
| | $(-)Y_{2\pm2}$ | $\frac{1}{3}$ |
| $W'_{1\downarrow}$ | $(-)Y_{2\pm1}$ | $\frac{2}{3}$ |
| | $(-)Y_{2\pm2}$ | $\frac{1}{3}$ |
| $L_{3\downarrow}$ | $(-)Y_{2\pm2}$ | $\frac{2}{3}$ |
| | $(-)Y_{20}$ | $\frac{1}{3}$ |
| $X_2$ | $(-)Y_{2\pm2}$ | $\frac{2}{3}$ |
| | $(-)Y_{20}$ | $\frac{1}{3}$ |
| $K_2$ | $(-)Y_{2\pm1}$ | $\frac{2}{3}$ |
| | $(-)Y_{2\pm2}$ | $\frac{1}{3}$ |

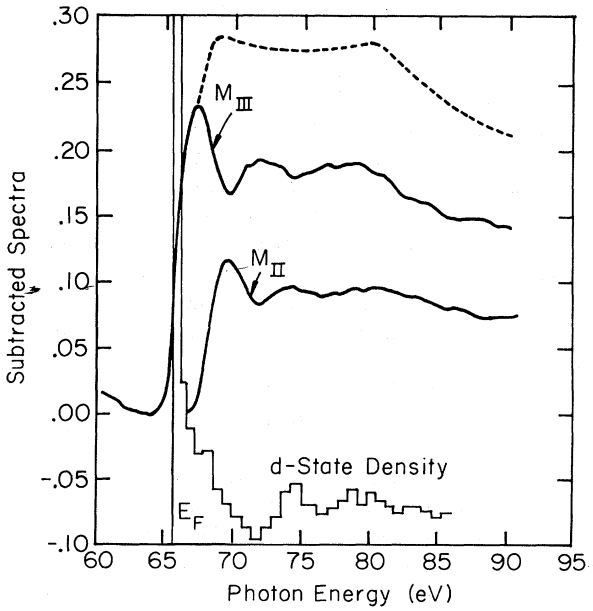


FIG. 2. Measured $M$ spectrum components of Ni compared with the component density of $d$ states above $E_F$ (Ref. 26).

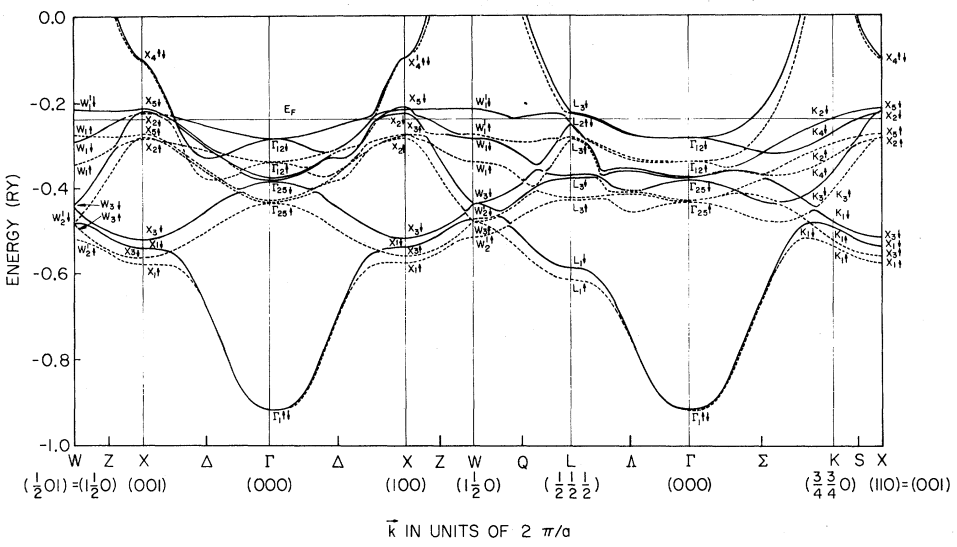


FIG. 3. APW bands for ferromagnetic nickel computed by Wang and Callaway (Ref. 8).

character conduction-band wave functions for states above the Fermi level. The appropriate conduction-band wave functions are basis functions corresponding to representations having $d$ symmetry in the APW bands for ferromagnetic nickel computed by Wang and Callaway,[8] shown in Fig. 3. The weights are the fraction of each character contained in the particular state.

From Fig. 3 and Table I, it is apparent that the minority spin states above the Fermi level have mainly symmetry corresponding to basis functions of both $Y_{2\pm1}$ and $Y_{2\pm2}$ spherical harmonics with relative weights

$$\mathfrak{W} = W\left|Y_{2\pm1}/Y_{2\pm2}\right| = 2, \tag{4}$$

where $W$ is the weight.

The matrix elements, Eq. (3), corresponding to dipole transitions produced by LCP and RCP light are given by Bethe and Salpeter.[29] For the case of interest here, we define

$$\begin{aligned} B &= \left|\langle Y_{10}|X+iY|Y_{21}\rangle\right|^2R^2 \\ &= \left|\langle Y_{10}|X-iY|Y_{2\text{-}1}\rangle\right|^2R^2 = (\tfrac{2}{5})R^2, \\ A &= \left|\langle Y_{11}|X+iY|Y_{22}\rangle\right|^2R^2 \\ &= \left|\langle Y_{1\text{-}1}|X-iY|Y_{2\text{-}2}\rangle\right|^2R^2 = (\tfrac{4}{5})R^2, \end{aligned} \tag{5}$$

where $R^2$ corresponds to the square of the dipole radial integral for $3p$-$3d$ wave functions.

With these definitions, the sum and differences of the matrix elements for LCP and RCP radiation corresponding to optical and magneto-optical absorption, respectively, are shown in Table II. As may be noted, $\sigma_{xy}^{(2)}$ is not much smaller than $\sigma_{xx}^{(1)}$, in contrast to the situation at visible wavelengths where $\sigma_{xy}^{(2)}$ is much smaller than $\sigma_{xx}^{(1)}$. As shown in Sec. IV, and as one might suspect, the magneto-optical effects are thus easily detectable in this case.

Figure 4 illustrates the results, including the energy dependence introduced by the density of final states. The density-of-states model, shown as an insert in Fig. 4, has been idealized from the calculated density of states of Fig. 1 associated with the bands shown in Fig. 3. In obtaining the results shown in Fig. 4, the spectra have been broadened using a 1.5-eV-width Gaussian function to more accurately simulate that which will be measured in an experiment. For simplicity, it has been assumed that the energy dependence of the density of states of the separate components of $Y_{2\pm2}$ and $Y_{2\pm1}$ are the same, although different energy dependence for each could easily be incorporated into the model.

In Fig. 4(a), the absorption spectrum produced by the sum of $\Delta m = \pm 1$ matrix elements for the $p_{3/2}\,p_{1/2}$ doublet is shown to consist of two peaks with weights in the ratio of 2:1 separated by the spin-orbit splitting $\Delta$, and to have shapes governed by the Gaussian-weighted unoccupied minority spin $d$-band density of states. This result corresponds to the basic result of Fig. 2, and describes the density-of-states modulation introduced into the x-

TABLE II. Predicted relative magnitudes of $\langle\sigma_{xx}^{(1)}\rangle$ and $\langle\sigma_{xy}^{(2)}\rangle$ for the $M_2$ and $M_3$ transitions in ferromagnetic nickel at full magnetic moment. In the last column, the value $B/A=\frac{1}{2}$ was used (see text). Brackets $\langle\rangle$ indicate the weight associated with the absorption.

| Transition | $\langle\sigma_{xx}^{(1)}\rangle$ (LCP+RCP) | $\langle\sigma_{xy}^{(2)}\rangle$ (LCP−RCP) | $\langle\sigma_{xy}^{(2)}\rangle/\langle\sigma_{xx}^{(1)}\rangle$ |
|---|---|---|---|
| $3P_{1/2}\rightarrow d$ | $\frac{2}{3}B+\frac{1}{3}A$ | $\frac{1}{3}A$ | $\frac{1}{2}$ |
| $3P_{3/2}\rightarrow d$ | $\frac{4}{5}B+\frac{2}{3}A$ | $-\frac{1}{3}A$ | $-\frac{1}{4}$ |

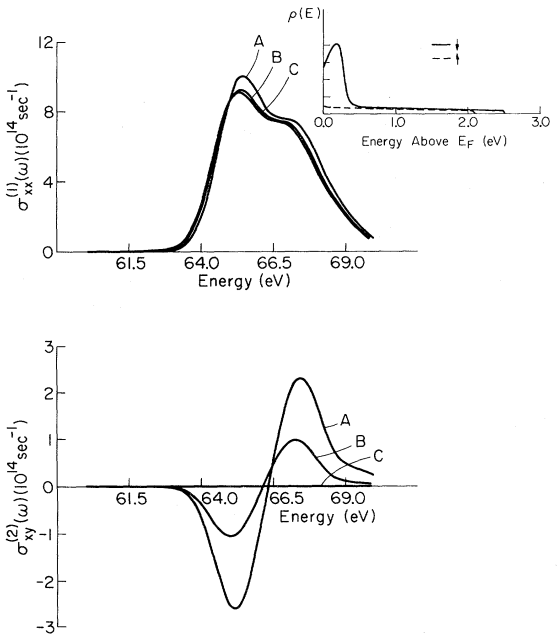


FIG. 4. Optical and magneto-optical absorption of the $M_{23}$ edge in nickel. Insert: density-of-states model for unfilled final $d$ states. A Gaussian with a 1.5-eV-wide full width at half-maximum was used to broaden the spectra. The curves $A$ correspond to full magnetic moment ($T=0$). Curves $B$ and $C$ correspond to Stoner model predictions for successively higher temperatures, $T=T_c$, for curve $C$.

ray absorption measurement.

The magneto-optical spectrum, corresponding to the difference of the $\Delta m=\pm 1$ matrix elements from the $p_{3/2}$ $p_{1/2}$ doublet of (7), is shown in Fig. 4(b). The net spin polarization of the final state in conjunction with spin-orbit splitting of the initial state produces two contributions of *equal* weight but with opposite sign, again separated by the spin-orbit splitting. The magneto-optical absorption results from the $A$ matrix elements, whereas the total absorption contains contributions from both $A$ and $B$ matrix elements.

The scale for $\sigma_{xx}^{(1)}(\omega)$ shown in Fig. 4 has been chosen so that the peak amplitude corresponds to the measured value for the linear x-ray absorption coefficient $\alpha$ at the nickel $M_{23}$ edge using the relation

$$\sigma_{xx}^{(1)}=\omega\epsilon_{xx}^{(2)}/4\pi=(\omega/4\pi)\,\alpha\lambda_0/2\pi\,,$$

where $\lambda_0$ is the x-ray wavelength in free space. The relationship between the scale of $\sigma_{xy}^{(2)}(\omega)$ and $\sigma_{xy}^{(1)}(\omega)$ is given in Table II.

Raising the temperature of the samples causes a decrease in the net magnetization and thus in the spin polarization of the sample. This decrease in net magnetization can occur in two distinct ways. One is a decrease in the Stoner exchange splitting which will raise the energy of the majority spins and lower the energy of the minority spins, as shown in Fig. 1, both relative to $E_F$. The second is by spin-wave excitations as discussed in the Introduction. These two mechanisms reflect themselves differently in the magneto-optic spectrum raising the exciting possibility of determining separately the variation of each with temperature.

The spin-wave excitation mechanism by itself, if no consequent decrease in exchange splitting occurs, will simply decrease the magnitude of magneto-optical absorption without changing its shape. A decrease in the Stoner exchange splitting will change the shape of the magneto-optical absorption spectrum. Changes in the ordinary optical spectrum are much weaker, and consequently are that much more difficult to detect and interpret.

Unfortunately, Ni is not an ideal case to illustrate this different variation between spin-wave and Stoner exchange splitting. The lifetime broadening of 1.5 eV is larger than the width of the main structure in the unoccupied $d$ band of about 0.4 eV. Thus the structure introduced by the density-of-states modulation is dominated by lifetime effects and would not show much narrowing as the unoccupied $d$ band narrows from its initial value with a decrease in exchange splitting. On the other hand, Fe and Co are even less desirable candidates owing to additional complications that result when unfilled majority spin band states are present.

Figure 4 also illustrates the predicted changes with temperature. For the ordinary absorption in Fig. 4(a), the predominant effect is a slight decrease in the peak amplitude along with the broadening required to maintain a constant area under the curve. For magneto-optic absorption in Fig. 4(b), the area of the positive and negative peaks decrease in proportion to the decrease in net magnetization.

If spin-wave effects dominate, the decrease is a simple scaling effect. If exchange splitting dominates, then there is a slight shift to lower energies in addition to the decrease as is apparent in Fig. 4. In the curves of Fig. 4, it was assumed that the Fermi energy remains fixed relative to the core states.

In closing this section, we note that the lifetime broadening effects in Ni are appreciably larger than one would expect from extrapolating measurements from nearby elements.[26] Also many-body effects in photoemission in Ni are particularly large compared to other metals.[27] Study of the magneto-optic effects may throw further light on the cause of this behavior.

## IV. DISCUSSION

The spectral dependence of the $M_{23}$ optical and magneto-optical absorption for nickel shown in Figs. 4(a) and 4(b) suggest a direct method for measuring the exchange splitting of conduction bands. The narrow width of the unoccupied portion of the nickel $d$ band and the relatively large spin-orbit splitting of the $3p$ core level along with the band-structure result of a predominately filled majority spin band in ferromagnetic nickel, represent somewhat of a unique case—one that can be used to advantage by application of magneto-optical methods.

The initial sign of the magneto-optical absorption at the $M_{23}$ edge will determine the spin polarization of $d$ state at the Fermi level. Although we have used the basic assumption of the Stoner model—that is, an exchange split majority and minority spin bands—in arriving at our predictions for the magneto-optical spectrum, the sign is model independent. An initial negative sign of $\sigma_{xy}^{(2)}$ at threshold corresponds uniquely to optical transitions to predominately minority spin states. The separation between positive and negative peaks in the magneto-optical absorption can be analyzed to obtain an accurate measure of the $3p$ core spin-orbit splitting.

The shapes as a function of photon energy of the magneto-optical spectrum contain information directly related to the local density of $Y_{2\pm2}$ character $d$ states; the degree to which the density-of-states influence the shape should be more direct than the case discussed in relation to Fig. 2. Here it was shown that analysis of the measured $M_{23}$ absorption based on a 2:1 ratio for contributions from the $p$ doublet resulted in reasonable agreement with theoretical $d$-band density of states if one neglects the absorption edge effects introduced by the photoelectron-core hole interaction.

It is interesting to note that extension of this technique to the $s$ core state offers a possibility of probing for spin polarization of $p$-character conduction-band states. In this case, the mechanism would involve spin-orbit coupling and spin polarization of the final $p$ state only, and the observed effect would, therefore, be very small, not only because of the reduced spin polarization and spin-orbit coupling strength of the $p$ band, but also because of the partial cancellation resulting from the large width of the $p$ band in relation to the spin-orbit coupling energy.[22] Based on the results of visible–near-uv magneto-optical measurements and the ratio of matrix elements for $3s$-core to $p$-conduction band, and $3d$–$p$ conduction-band transitions, plus the relative spin-orbit coupling strengths involved, magneto-optical effects associated with $3s$-core transitions would be on the order of one part in $10^5$. In the soft-x-ray range, this approaches the currently available resolution. On the other hand, a signal if detected would allow one to estimate the $p$-band spin polarization, which could have bearing on the spin-polarized electron emission results.

We conclude by turning to a brief discussion of the prospects for obtaining experimental results for the $M_{23}$ magneto-optical spectra with sufficient accuracy to check our predictions. A synchrotron radiation source, such as the facility at Stoughton, Wisc., or at the Stanford Linear Accelerator Laboratory would be an ideal source. The radiation from these sources is highly stable, and polarized, having useful intensity extending from the infrared range into the x-ray range. The characteristic of synchrotron radiation over the useful wavelength range has been well established by theoretical work and practical experience gained in the many experiments that have been conducted using storage-ring sources.[30]

The spectral resolution that can be achieved in the energy range corresponding to the $M_{23}$ edge of nickel (just above 65 eV) is more than adequate to resolve the predicted structure. Gahwiller and Brown[31] report an over-all instrument bandwidth of 0.04 eV at 70 eV using a 2-m grazing incidence monochromator having a 576-lines/mm grating and 10-$\mu$ slits. This resolution is considerably better than the energy resolution available using photoemission techniques which are limited by the accuracy that the emitted electrons can be energy analyzed. With the spectrometer operating at 0.04-eV resolution, changes in optical density (or changes in reflectance) of the order of $2\times10^{-5}$ can be measured. The sensitivity can be improved at the expense of reduced-wavelength resolution.

We can estimate the approximate magnitude of the parameters that would be measured in an experiment using the results of Fig. 4. In the polar configuration, the rotation and ellipticity for reflected and transmitted light are described by a complex number $\phi = \theta + i\epsilon$ that is related to elements of $\tilde{\sigma}$ by the expressions

$$\phi = -i\epsilon_{xy}/\epsilon_{xx}^{1/2}(\epsilon_{xx}-1) \quad \text{(reflection)}, \tag{6}$$

$$\phi = -\pi(\Delta x/\lambda_0)(\epsilon_{xy}/\epsilon_{xx}^{1/2}) \quad \text{(transmission)}, \tag{7}$$

where

$$\sigma_{ij} = (i\omega/4\pi)(\epsilon_{ij}-\delta_{ij}),$$

$\Delta x$ is the thickness and $\lambda_0$ is the free-space wavelength. The corresponding formulas for oblique incidence in the longitudinal and transverse configurations contain the same basic feature: The

transmission effects depend on the ratio of off-diagonal to square root of diagonal components multiplied by the thickness, and the reflection effects correspond to an effective path length

$$\Delta x_{\text{eff}} \cong (\lambda/\pi)\left|\epsilon_{xx}-1\right|^{-1} .$$

If we assume a thickness $\Delta x$ corresponding to attenuation of $1/e$ at the nickel $M_{23}$ edge ($\Delta x = \alpha^{-1} = 1.2\times10^{-6}$ cm) and values of Table II, the results of Fig. 4 produce values of $\phi$ of the order of a degree. This is very large compared with results measured in the visible wavelength range. Corresponding large changes in reflected intensity (of the order of $10^{-1}$) are predicted for the transverse configuration. Our model assumes that there is no appreciable overlap of the positive and negative absorption peaks produced by broadening effects, and the magnitude of measured parameters could clearly be reduced in proportion to the overlap caused by broadening. The intrinsic broadening of the $M_{23}$ edge is estimated to be on the order of[27] 1.5 eV; with a $3p$ spin-orbit splitting of 2.25 eV, the overlap should be small, justifying our assumptions.

In summary, we predict strong magneto-optical effects will be observed at the $M_{23}$ edge of nickel. These effects should be easily measurable using synchrotron-radiation sources. The resulting spectra will contain electronic structure information that include the spin-orbit splitting of the $3p$ core state, the spin-polarization of the unfilled conduction-band $d$ states, and perhaps information about the shape of the $d$-band density of states above the Fermi level if the lifetime broadening is much less than estimated. A study of the temperature dependence of the $M_{23}$ magneto-optical absorption spectra of ferromagnetic metals provides the exciting possibility to separately measure the contribution of the two mechanisms that decrease the magnetization—the variation of the exchange splitting and the excitation of spin waves.

*Supported in part by the Office of Naval Research under Grant No. N00014-67-A-0305-0027.

†Supported in part by the Air Force Office of Scientific Research.

[1]P. Weiss, J. Phys. 6, 667 (1907).

[2]W. Heisenberg, Z. Phys. 49, 619 (1928); J. H. Van Vleck, J. Chem. Phys. 6, 105 (1938).

[3]E. C. Stoner, Proc. Roy. Soc. Lond. A 165, 372 (1938); C. Herring and C. Kittel, Phys. Rev. 81, 869 (1951).

[4]M. C. Gutzwiller, AIP Conf. Proc. 10, 1197 (1972).

[5]A. V. Gold, J. Low Temp. Phys. 16, 112, 3 (1974).

[6]A. P. Cracknell, Adv. Phys. 20, 1 (1971).

[7]J. L. Erskine and E. A. Stern, Phys. Rev. Lett. 30, 1329 (1973); B. R. Cooper, Phys. Rev. 139, A1504 (1965).

[8]C. S. Wang and J. Callaway, Phys. Rev. B 9, 4897 (1974).

[9]R. Moon, Phys. Rev. 136, A195 (1964); H. A. Mook, *ibid.* 148, 495 (1966).

[10]E. P. Wohlfahrth, in *Proceedings of the International Conference on Magnetism, Nottingham, England*, 1964 (The Institute of Physics and The Physical Society of London, England, 1965), p. 51.

[11]D. J. Pierce and W. E. Spicer, Phys. Rev. B 6, 1787 (1972); C. S. Fadley and D. A. Shirley, Phys. Rev. Lett. 21, 980 (1968).

[12]J. L. Rowe and J. C. Tracy, Phys. Rev. Lett. 27, 799 (1971); A. J. McAlister, J. R. Cuthill, R. C. Dobbyn, M. L. Williams, and R. E. Watson, *ibid.* 29, 179 (1972).

[13]H. A. Mook, J. W. Lynn, and R. M. Nicklow, Phys. Rev. Lett. 30, 556 (1973).

[14]J. B. Sokoloff, Phys. Rev. Lett. 31, 1417 (1973); R. E. Prange and V. Korenman, AIP Conf. Proc. 24, 324 (1975).

[15]G. Busch, M. Campagna, and H. C. Siegmann, Phys. Rev. B 4, 746 (1971).

[16]P. M. Tedrow and R. Meservey, Phys. Rev. B 7, 318 (1973); and Phys. Rev. Lett. 26, 192 (1971).

[17]H. C. Siegmann, Phys. Lett. C 17, 2, 37 (1975).

[18]E. P. Wohlfahrth, Phys. Lett. 36, 131 (1971); P. W. Anderson, Philos. Mag. 24, 203 (1971); S. Doniach, AIP Conf. Proc. 5, 549 (1972).

[19]J. L. Erskine, E. A. Stern, Phys. Rev. Lett. 30, 1329 (1973).

[20]G. Lonzarich and A. V. Gold, Can. J. Phys. 52, 694 (1974); D. M. Edwards, *ibid.* 52, 704 (1974).

[21]H. S. Bennett and E. A. Stern, Phys. Rev. 137, A448 (1965).

[22]J. L. Erskine and E. A. Stern, Phys. Rev. B 8, 1239 (1973).

[23]P. N. Argyres, Phys. Rev. 97, 334 (1955); Y. R. Shen, *ibid.* 133, A511 (1964); J. Halpern, B. Lax, and Y. Nishina, *ibid.* 134, A140 (1964).

[24]D. J. Nagel, in *Proceedings of the International Conference on Band Structure Spectroscopy of Metals and Alloys*, edited by D. J. Fabian and L. M. Watson (Academic, New York, 1971), p. 457.
G. Wiech, Vol. 2, p. 51.

[25]D. J. Nagel, D. A. Papaconstantopoulos, and J. W. McCaffery, in *Proceedings of the International Symposium on x-ray Spectra and Electronic Structure of Matter*, Munich, 1972, edited by A. Saessler and G. Wiech, Vol. 2, p. 51.

[26]F. C. Brown, in *Solid State Physics*, edited by H. Ehrenreich, F. Sietz, and D. Turnbull (Academic, New York, to be published).

[27]S. Hüfner and G. K. Wertheim, Phys. Rev. B (to be published).

[28]A. Kotani and Y. Toyazawa, J. Phys. Soc. Jpn. 35, (1073); 35, 1082 (1973).

[29]H. Bethe and E. Salpeter, *Quantum Mechanics of One- and Two-Electron Atoms* (Springer-Verlag, New York, 1957).

[30]E. M. Rowe, R. A. Otte, C. H. Pruett, and J. D. Steben, IEE Trans. Nucl. Sci. 3, 159 (1969); also see, J. L. Erskine and E. A. Stern, Phys. Rev. B 8, 1239 (1973).

[31]C. Gähwiller and F. C. Brown, Phys. Rev. B 2, 1918 (1970).